Supplement to: Understanding Changes in Iceland's Streamflow Dynamics in Response to Climate Change

Hordur B. Helgason[1,2], Andri Gunnarsson[2], Óli G. B. Sveinsson[2], Bart Nijssen[1]

[1]Department of Civil and Environmental Engineering, University of Washington, Seattle, USA
[2]Hydropower Division, Landsvirkjun, Reykjavík, Iceland

Correspondence to: Hordur B. Helgason (helgason@uw.edu)

S1 Homogeneity analysis of streamflow series

To assess the homogeneity of streamflow records from the LamaH-Ice dataset, we performed the standard Petitts's test (Pettitt, 1979). The homogeneity analysis revealed that one timeseries needed to be omitted. Our approach to considering or omitting inhomogeneous series aligns with that of the Norwegian Water Resources and Energy Directorate's method for selecting reference streamflow series for climate change studies (Fleig et al., 2013). The analysis, including the justification for each streamflow series, is described here.

Pettitt's test (Pettitt, 1979) is a non-parametric change-point detection test derived from the Mann-Whitney two-sample test. We computed Pettitt's test for each streamflow gauge using the PyHomogeneity Python package (Hussain et al., 2023), setting the significance level at 0.05 and the number of Monte Carlo simulations used to approximate the significance of the test at 20,000. We applied the test to series for annual average streamflow, temperature and precipitation series. In cases where the test indicated a change-point in annual average streamflow, we manually inspected the streamflow series for breaks in homogeneity that were either 1) linked to a documented change in measurement practices or to incidents that compromised data quality, or 2) distinctly observable in the data, and these breaks could not be accounted for by breaks in temperature or precipitation. The streamflow series with inhomogeneity detected are shown below (Figures S1 to S16) along with reasoning for omitting or keeping the series in the trend analysis.

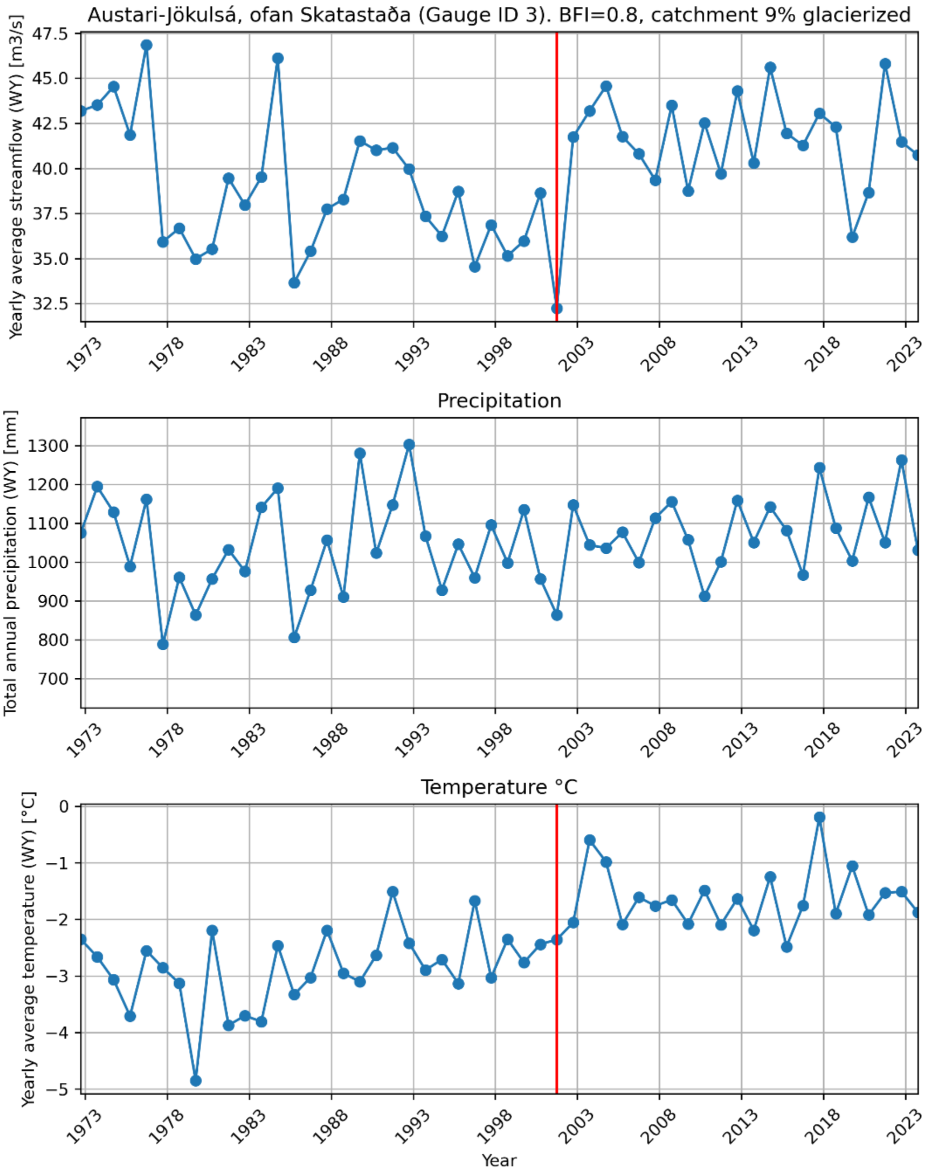

Figure S1: Austari-Jökulsá is a glacial river. A break in homogeneity is detected in the streamflow series in year 2000. The homogeneity break appears to be due to an increase in temperature, leading to increased glacier melt. The series is thus not omitted.

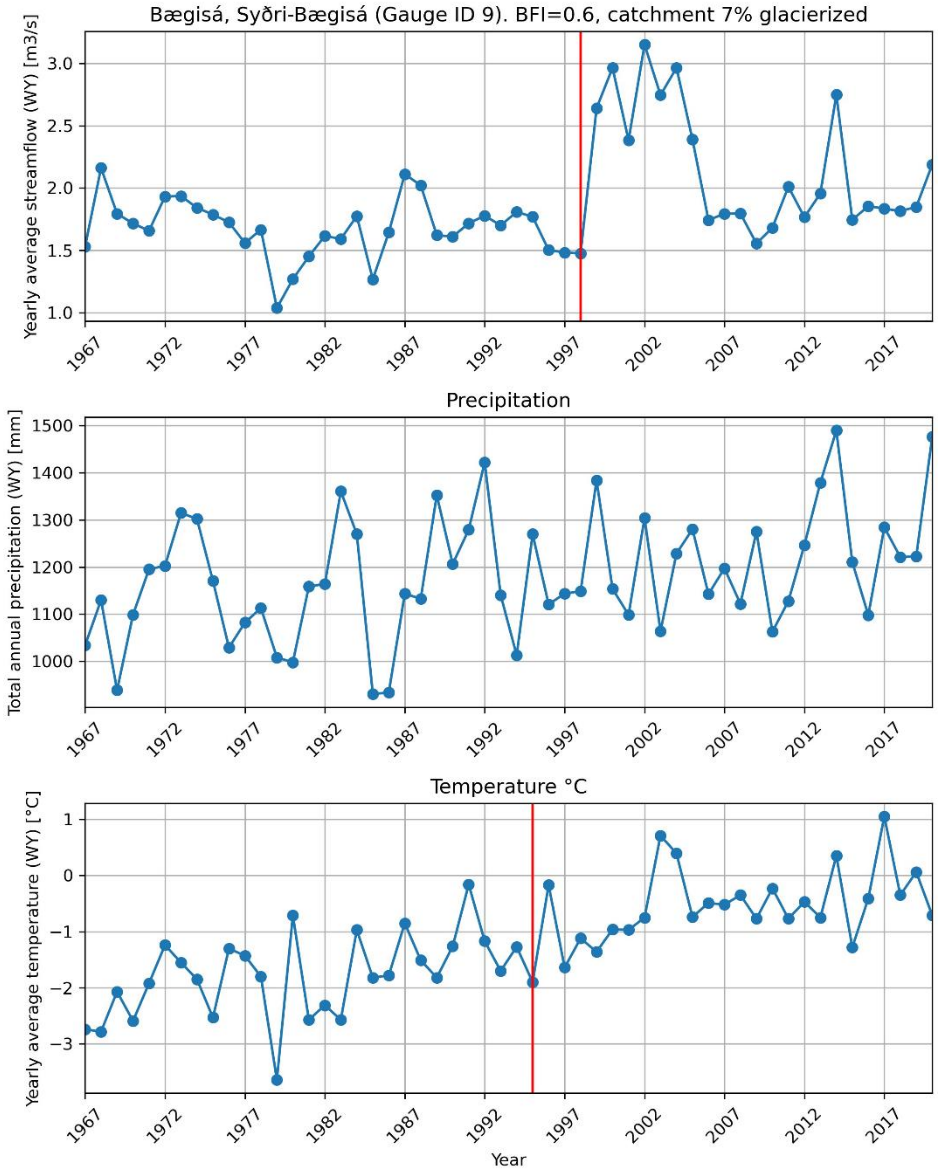

Figure S2: Syðri Bægisá: A break in homogeneity is found in the streamflow series in 1998. The high flow between 1999 and 2004 does not seem to be explained by changes in precipitation. The streamflow gauge is often interrupted by snow and ice in the winter and spring (Hróðmarsson and Þórarinsdóttir, 2018)**. The series is thus omitted from our analysis.**

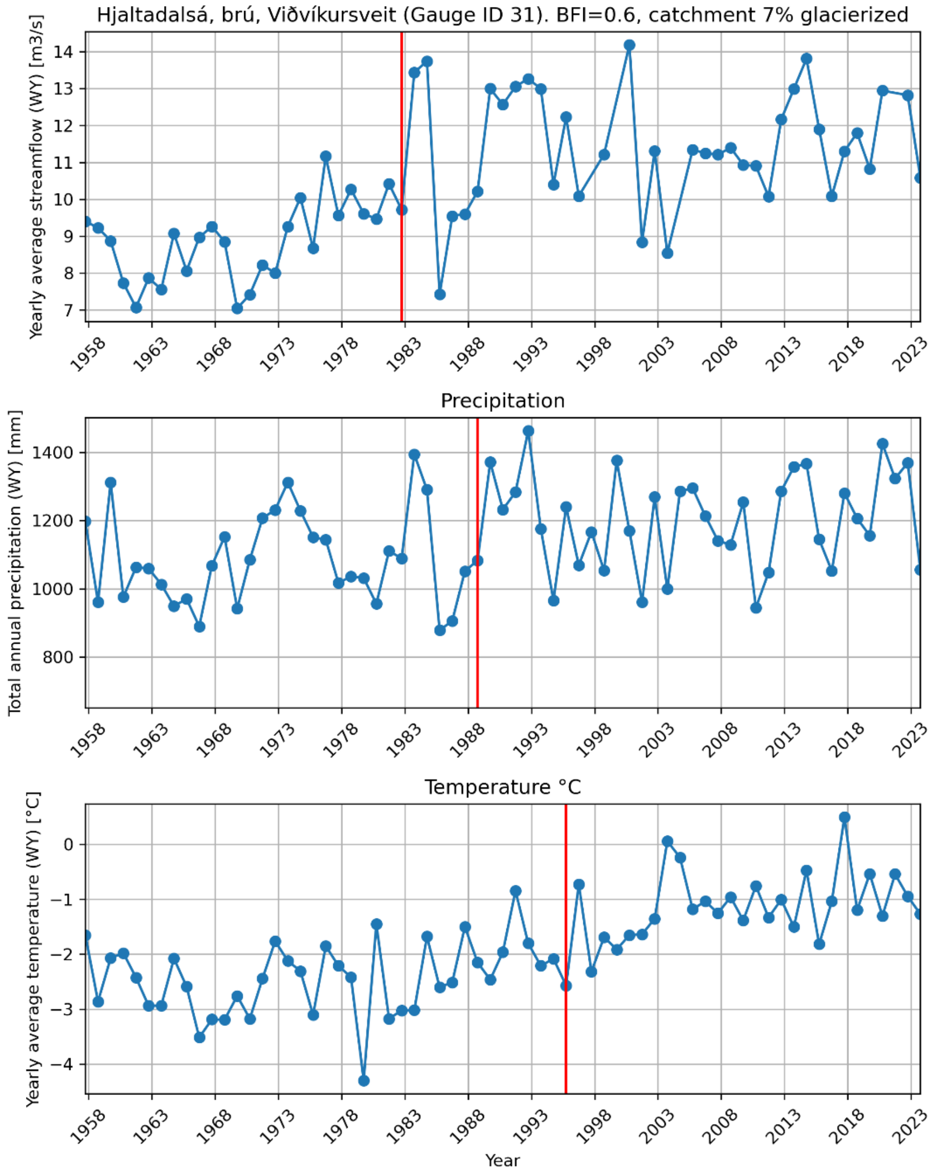

Figure S3: Hjaltadalsá: The break in homogeneity in streamflow (in year 1982) happens at a similar time as a break in precipitation series (1990). The general behaviour of the streamflow series is similar to that of the precipitation series. It is also possible that elevated streamflow after 1979 could be due to increased glacier melt due to higher temperatures. The series is thus not omitted.

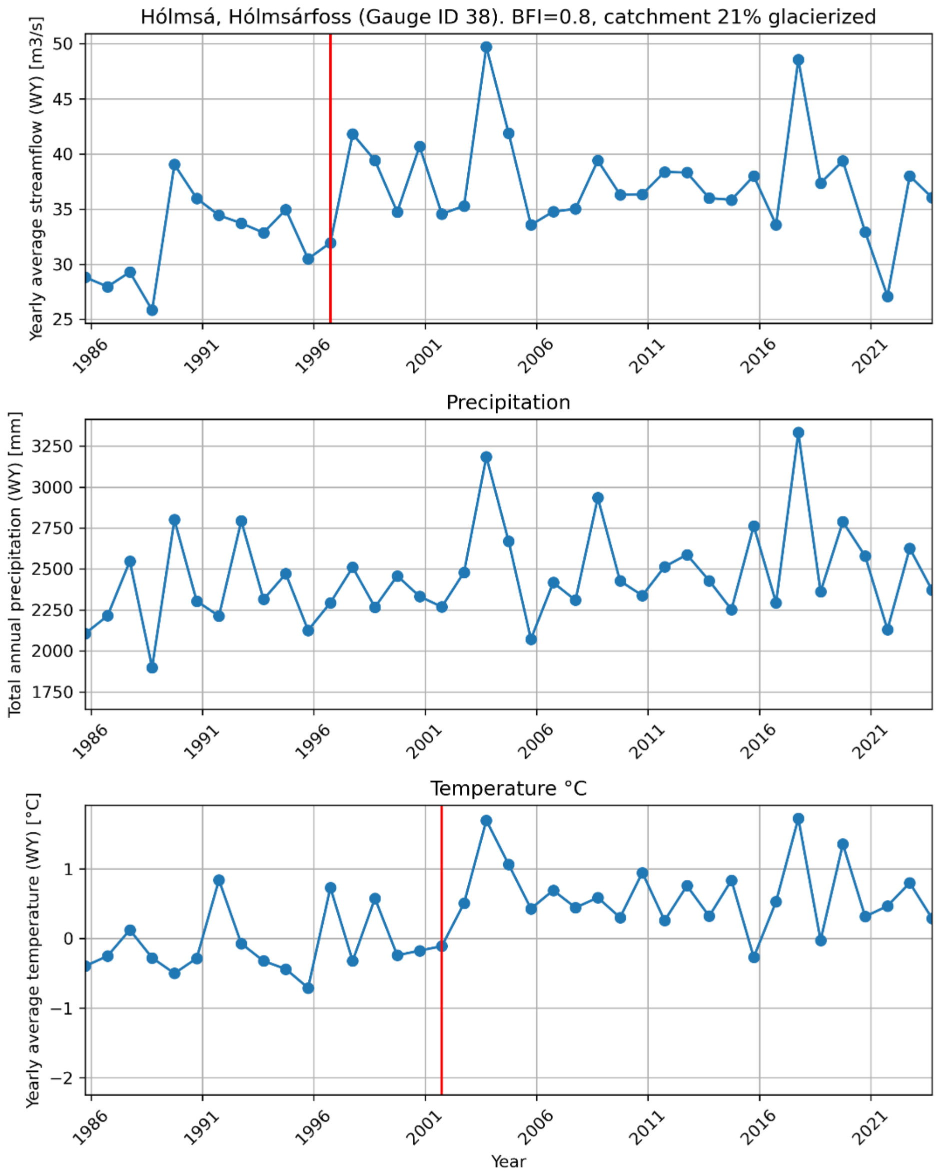

Figure S4: The break in homogeneity in streamflow (in year 1997) happens at a similar time as a break in the temperature series (year 2002), which suggests that the break is caused by increased glacier melt. The catchment has a glaciation of 21% in 2019. The series is thus not omitted.

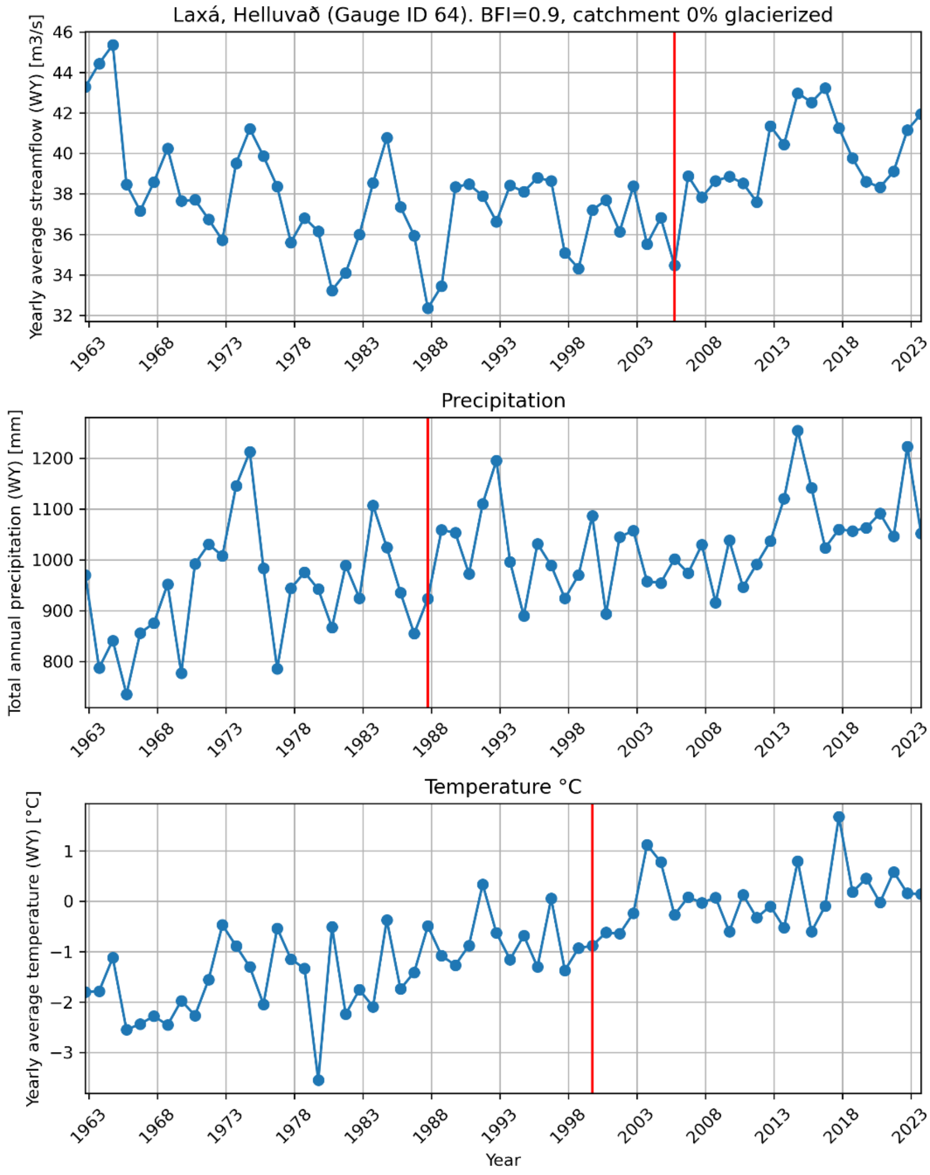

Figure S5: For Laxá river at Helluvað, a break in homogeneity is found in year 2005. Although breaks are found in the precipitation series (1987) and temperature series (1990), these breaks are not close enough in time to explain the streamflow break. The river has a high contribution of baseflow (BFI 0.9). The topographical watershed of Laxá river does not extend to the Dyngjujökull glacier, but the groundwater that flows to the river is likely to originate at the glacier. The increase in measured streamflow in the period 2006-2017 is most likely due to an increase in precipitation in the watershed and perhaps also partly explained by increased glacier melt at Dyngjujökull glacier. An analysis of groundwater level measurements in wells in the watershed, as well as streamflow in the Svartá river (gauge ID 83), confirms that the increase in streamflow/groundwater height after 2006 is real and thus the gauge is not omitted.

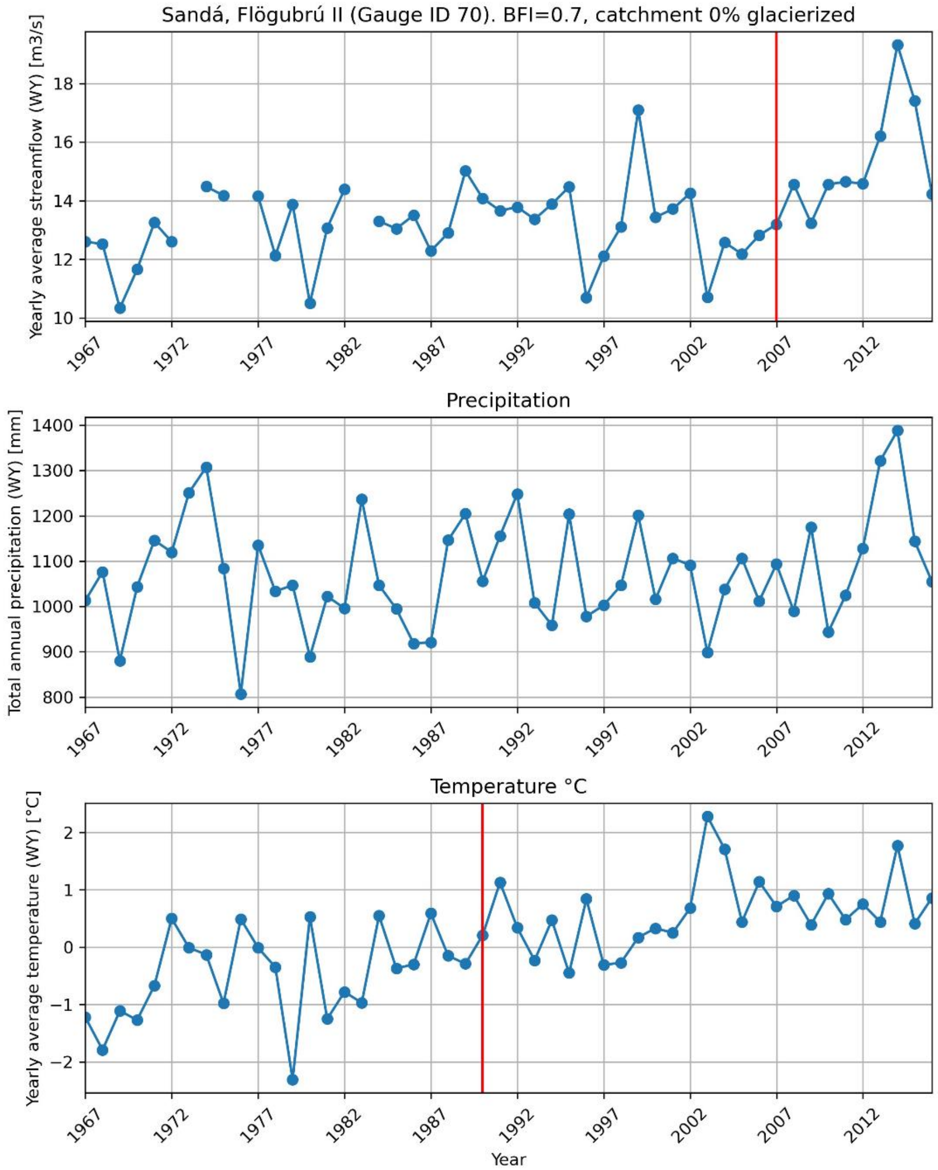

Figure S6: Sandá river at Flögubrú: Pettitt's test indicates a break in the streamflow series in 2007. As can be seen in the precipitation plot, the increase in streamflow after 2007 can most likely be explained by increases in precipitation. Therefore, we do not omit the series.

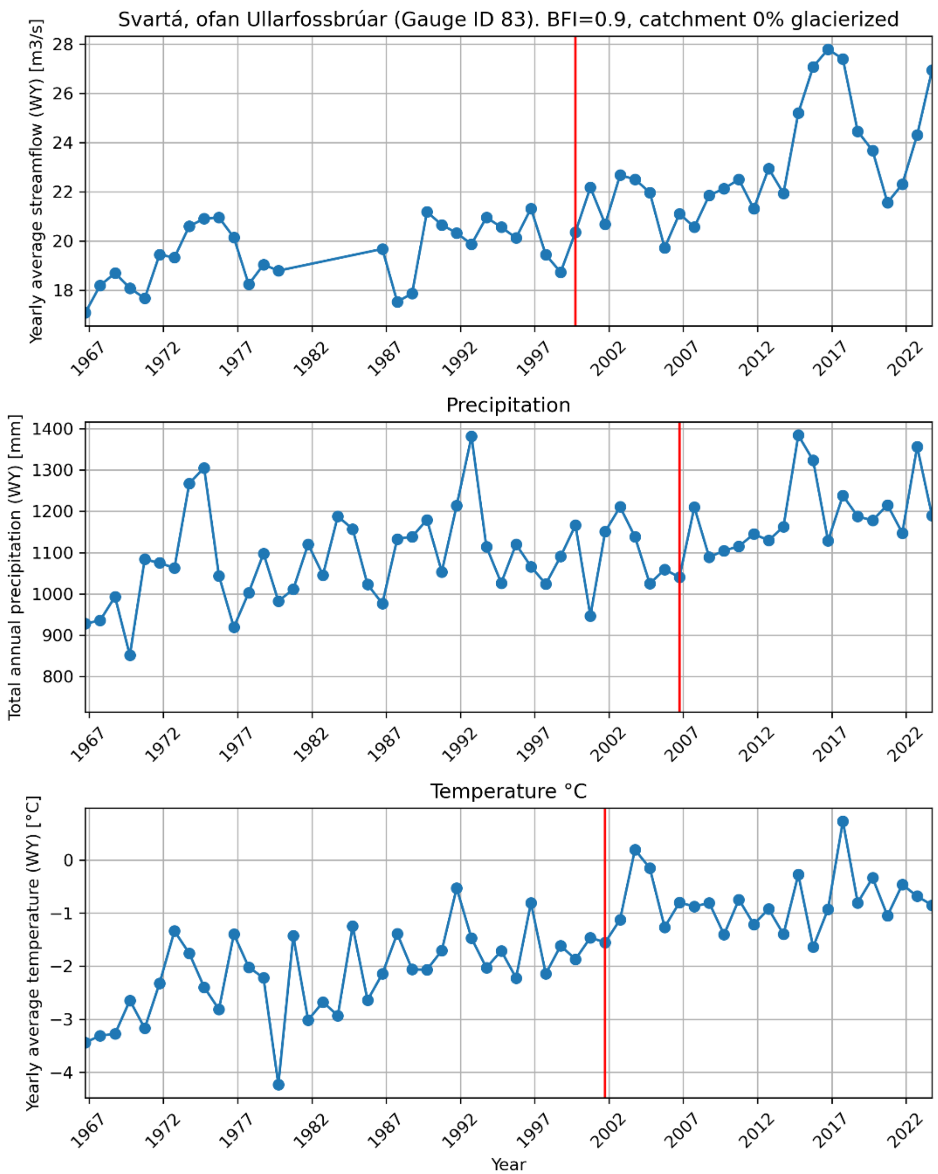

Figure S7: For Svartá river, a break in homogeneity is found in year 1999. A break is also found in the temperature series, in 2001, and precipitation, in 2006. The river has a high contribution of baseflow (BFI 0.9). The topographical watershed of Svartá river does not extend to the Dyngjujökull glacier, but the groundwater that flows to the river is likely to originate at the glacier. The increases in measured streamflow after the turn of the century is most likely due to an increase in precipitation in the watershed and/or increased glacier melt at Vatnajökull glacier. An analysis of groundwater level measurements in wells in the watershed, as well as streamflow in the nearby Laxá river (gauge ID 64), confirms that the increase in streamflow/groundwater height after 2007 is real and thus the gauge is not omitted.

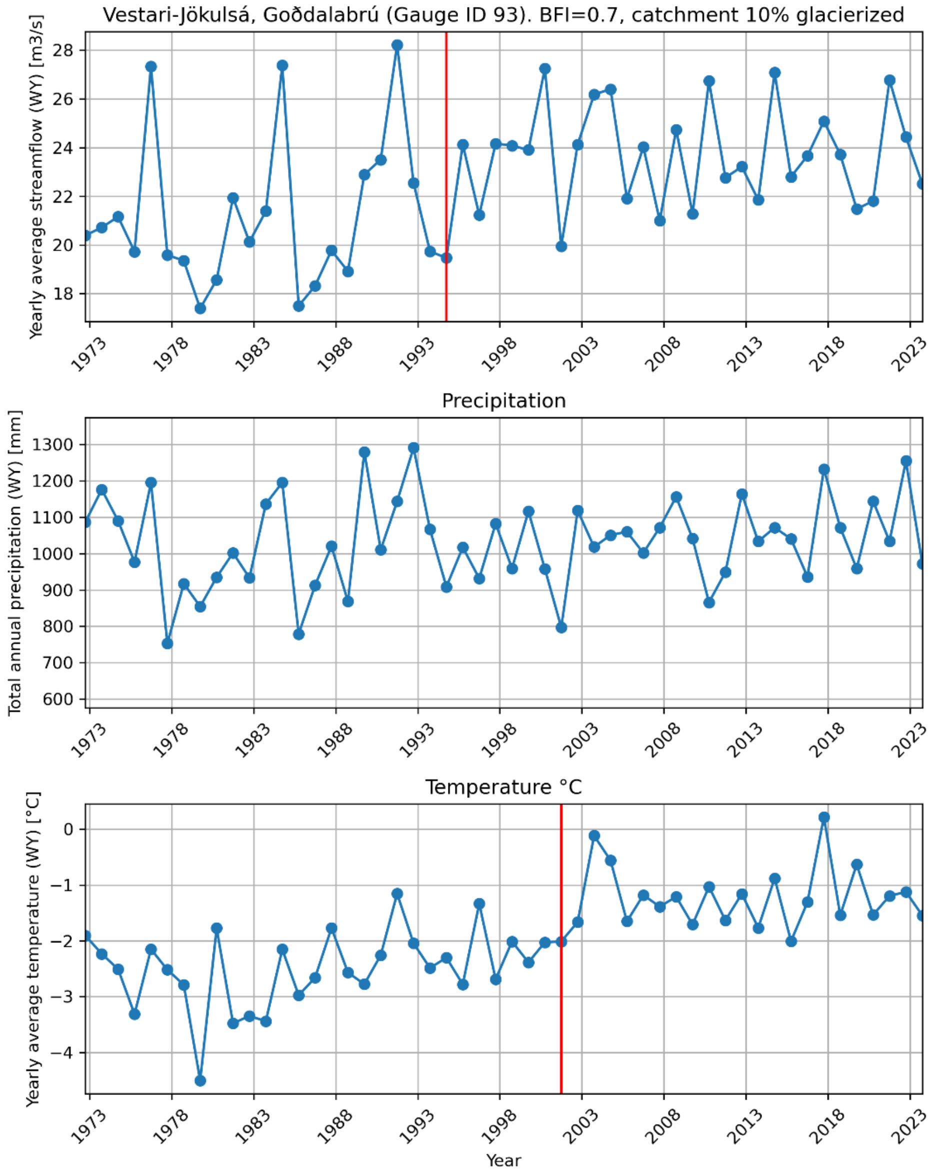

Figure S8: Vestari-Jökulsá river at Goðdalabrú is a glacial river. Pettitt's test indicates a break in the streamflow series in 1994. As can be seen in the temperature plot, the period before 2000 is much colder than latter parts of the series. The break in streamflow is most likely due to increased glacier melt, even if the homogeneity break in temperature is found in 2001. Therefore, we do not omit the series.

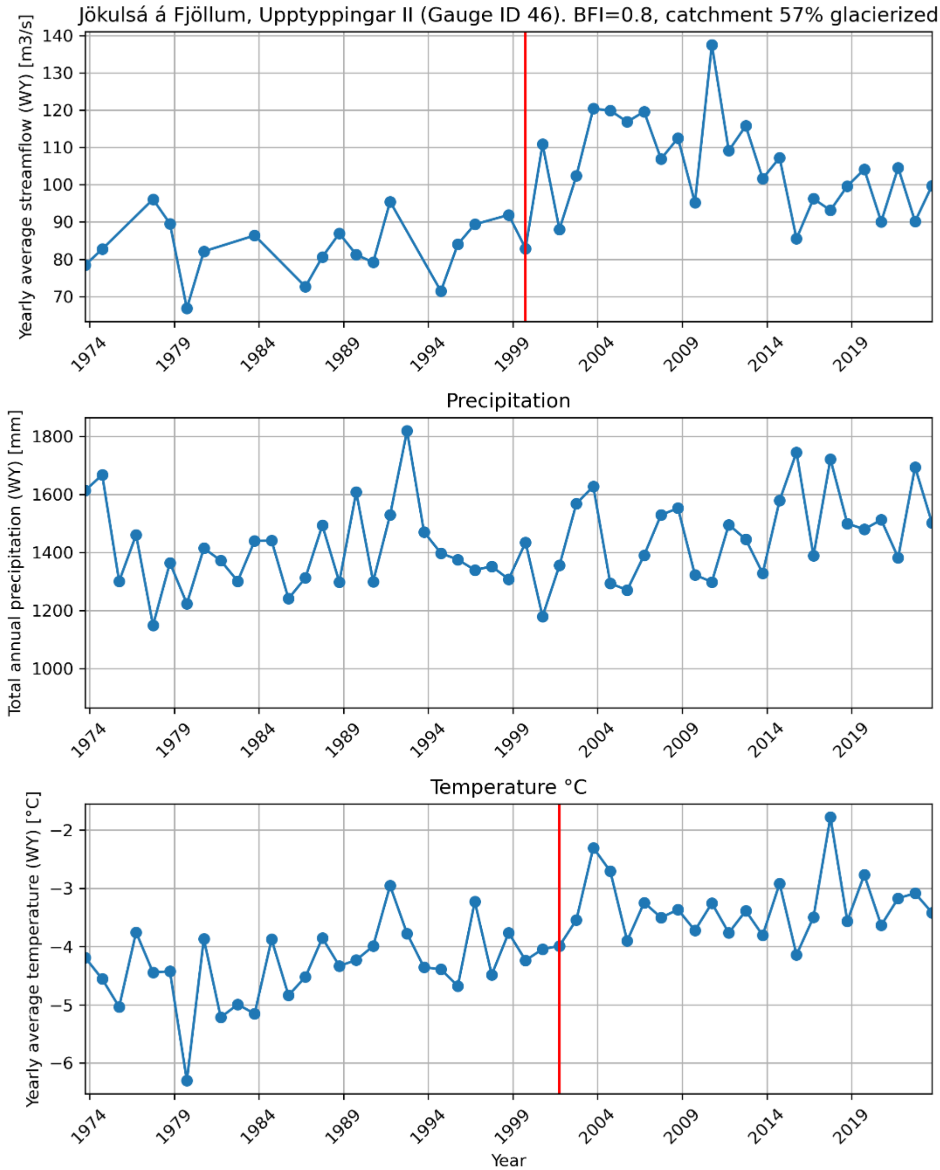

Figure S9: Jökulsá á Fjöllum is a glacial river. Pettitt's test indicates a break in the streamflow series in 1999. As can be seen in the temperature plot, the period before 1999 is colder than latter parts of the series. The break in streamflow is most likely due to increased glacier melt. Therefore, we do not omit the series.

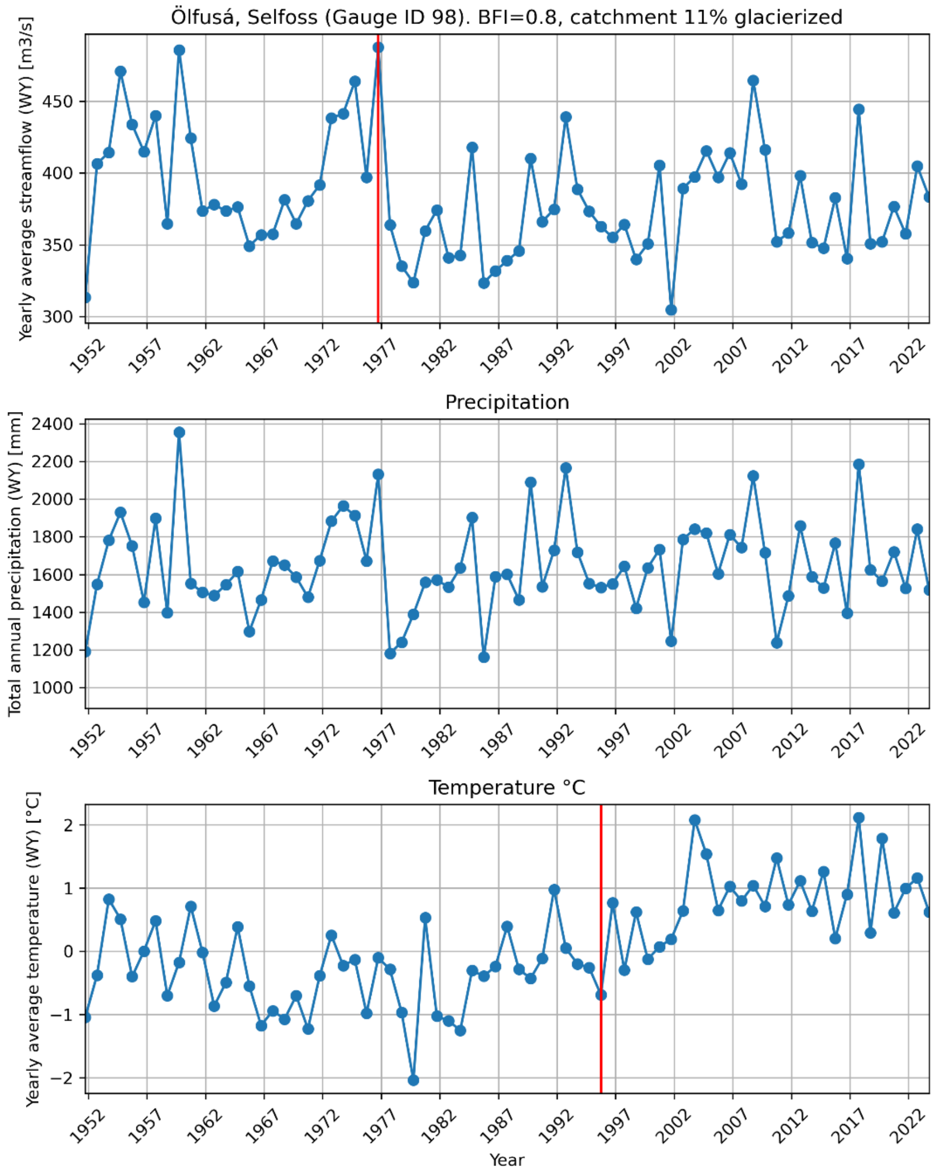

85 **Figure S10: Ölfusá is a glacial river with a high baseflow component. Pettitt's test indicates a break in the streamflow series in 1976, with higher streamflow in the period before that. The precipitation is also high in the period before 1976. Figure S12 shows a double-mass-curve where the streamflow in Ölfusá is compared to the streamflow in an upstream tributary, Brúará.**

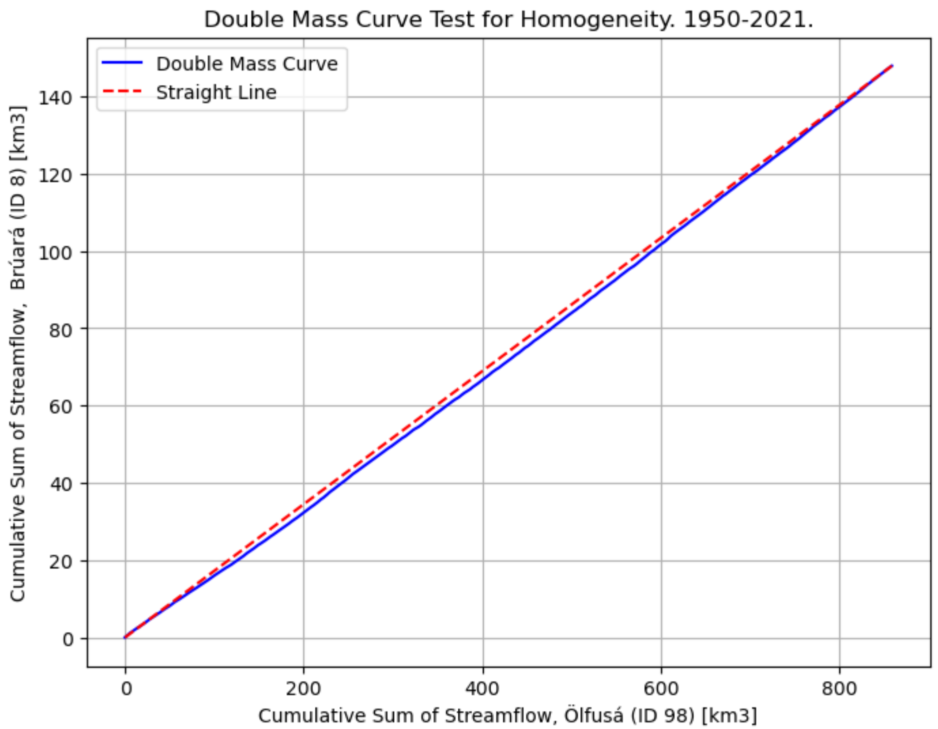

Figure S11: A double-mass-curve where cumulated streamflow in Ölfusá and Brúará are compared. The close fit to a straight line indicates that there is not a break in homogeneity in the streamflow series. The Ölfusá river is thus not omitted from the trend analysis.

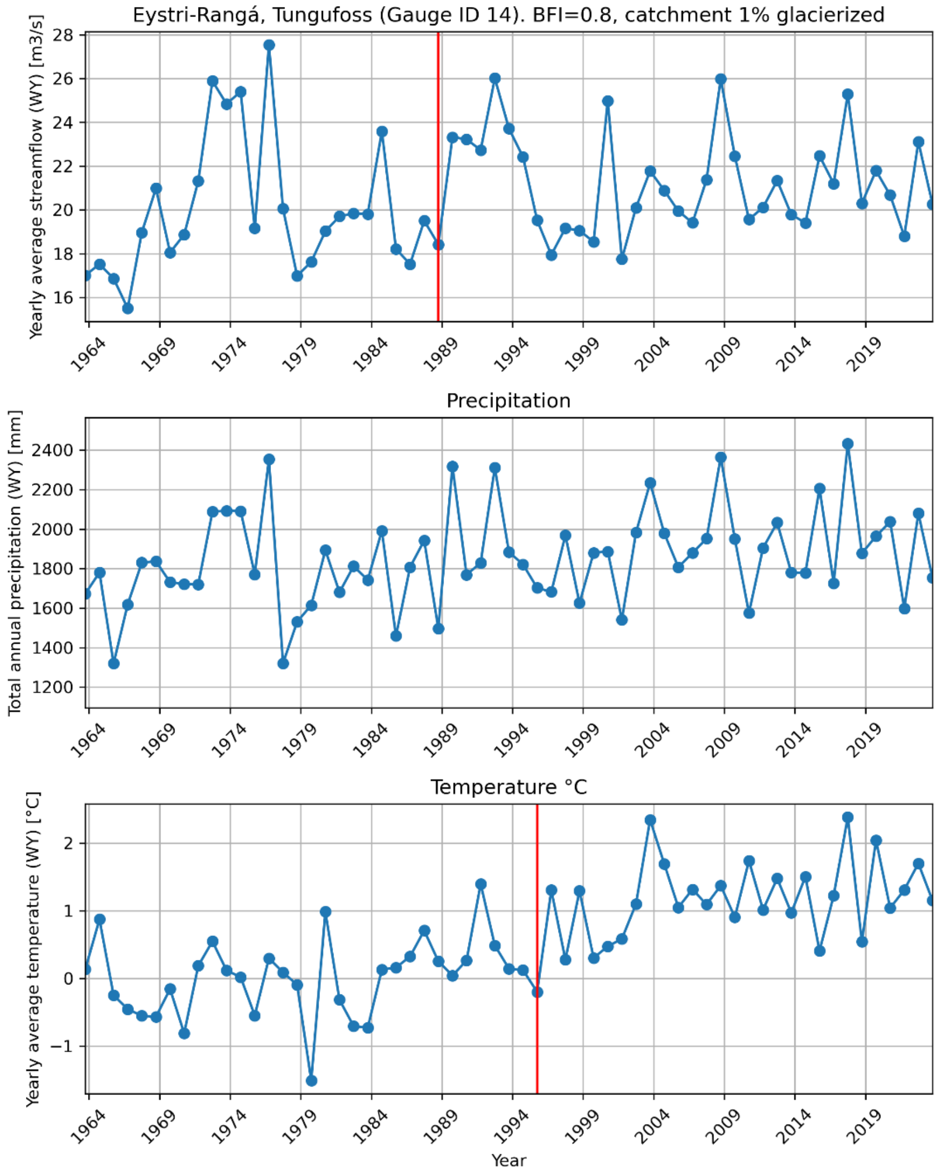

Figure S12: The streamflow in the river Eystri-Rangá shows a homogeneity break in 1988. The river is strongly influenced by baseflow, and the streamflow series shows a high similarity to the precipitation series, although the precipitation shows no break in homogeneity. The data from the streamflow gauge is of high quality and ice disturbances minimal (Hróðmarsson and Þórarinsdóttir, 2018)**. We do thus not omit the series.**

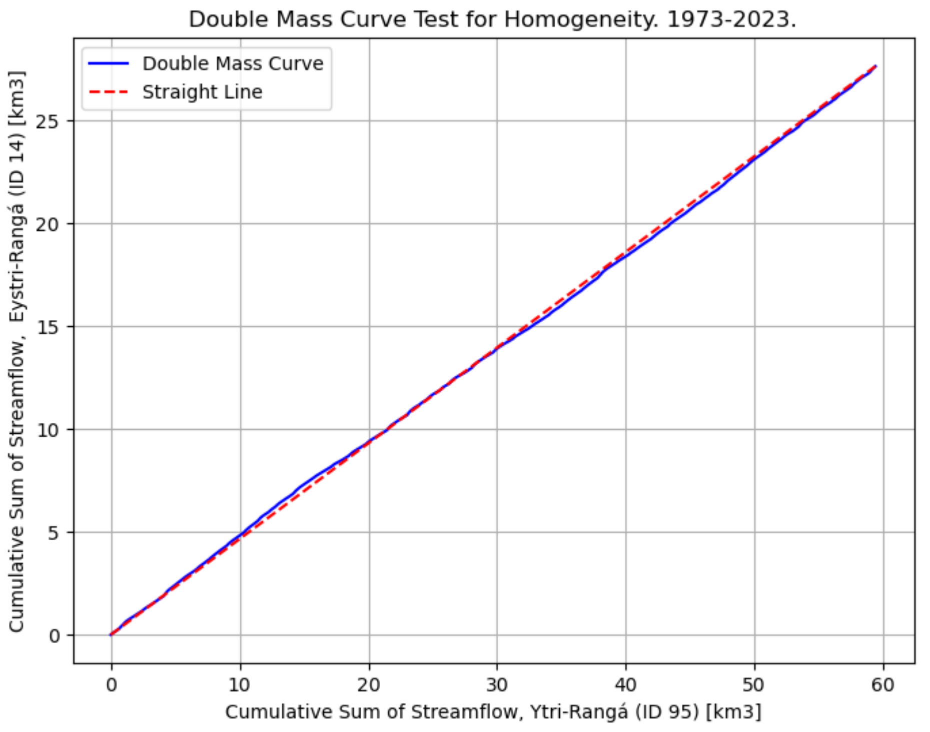

Figure S13: A double-mass-curve where cumulated streamflow in Ytri-Rangá and Eystri-Rangá are compared. The close fit to a straight line indicates that there is not a break in homogeneity in the streamflow series. The series from Eystri-Rangá river is thus not omitted from the trend analysis.

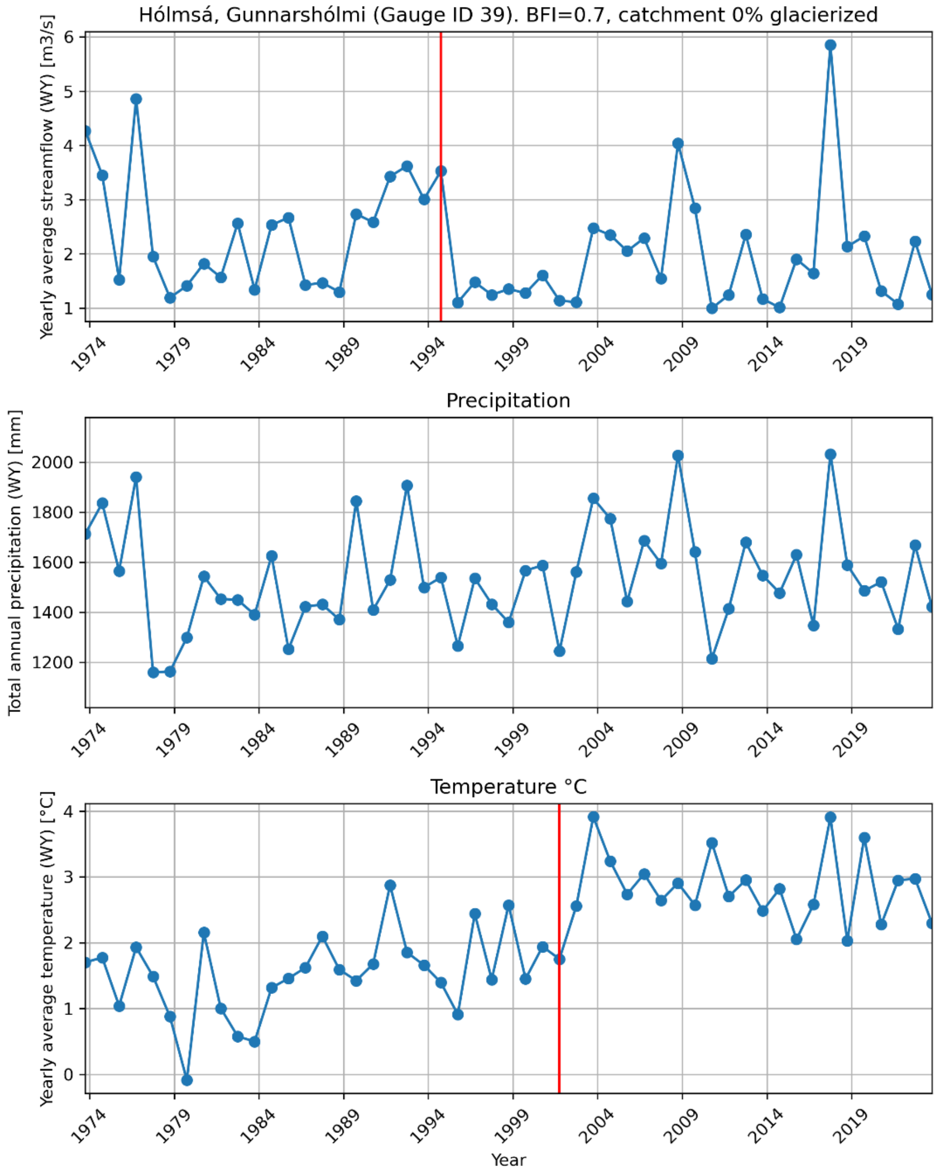

Figure S14: The streamflow in the river Eystri-Rangá shows a homogeneity break in 1995. A double-mass curve analysis is shown in Figure S15.

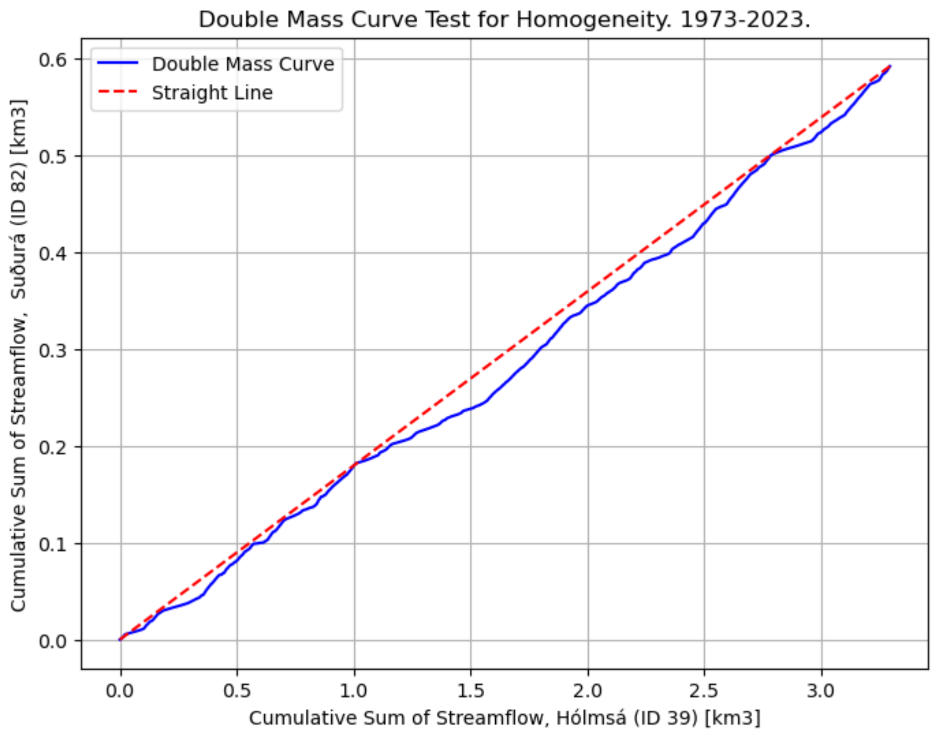

Figure S15: A double-mass-curve where cumulated streamflow in Hólmsá and the nearby Suðurá are compared. The close fit to a straight line indicates that there is not a break in homogeneity in the streamflow series. The series from the Hólmsá river is thus not omitted from the trend analysis.

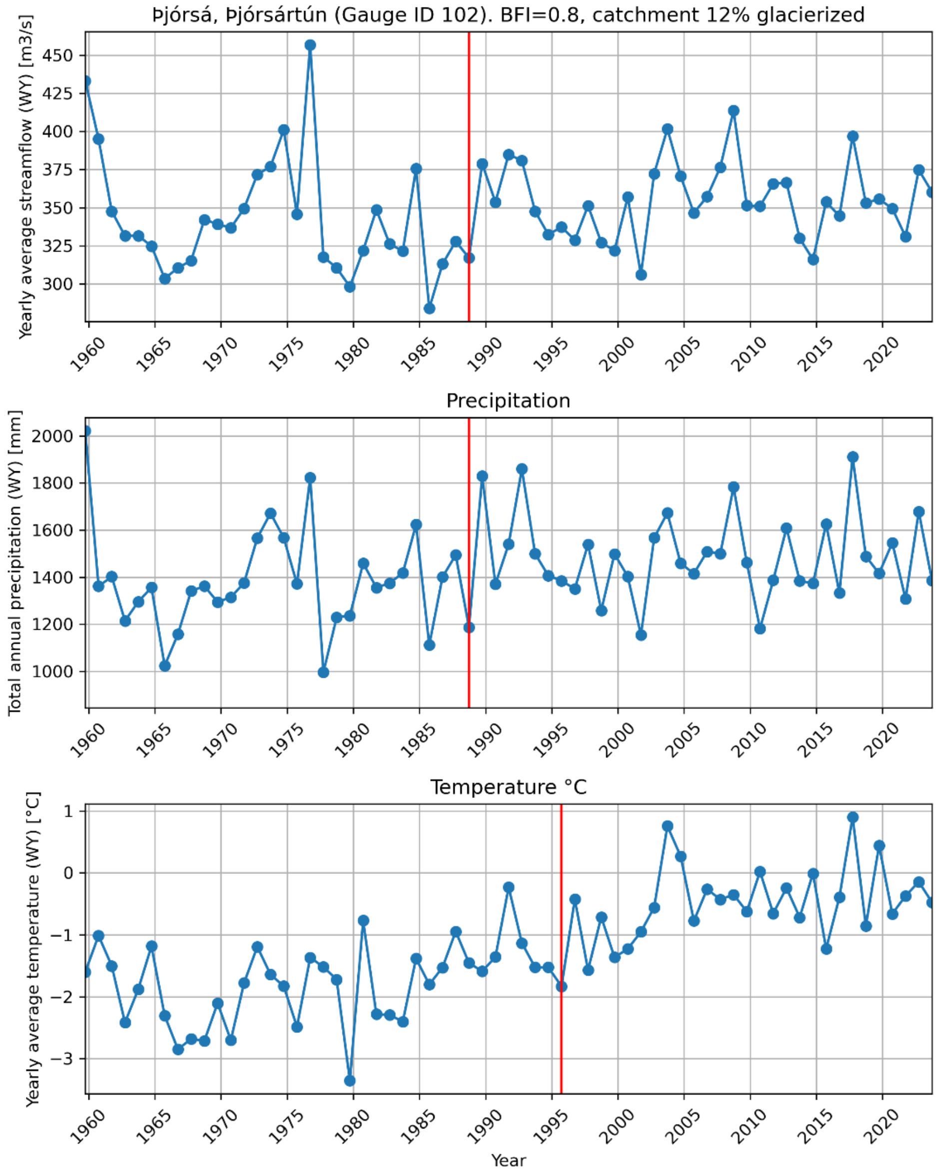

Figure S16: The Þjórsá rivers shows a break in homogeneity in 1988. Both precipitation and temperature are higher after that time. We thus assume that the break in homogeneity is explained by increases in precipitation and glacier melt due to higher temperatures.

S2 Changes in evapotranspiration compared to changes in precipitation

Figure S17 shows Figure 4 from the manuscript, with the units mm/decade instead of %/decade.

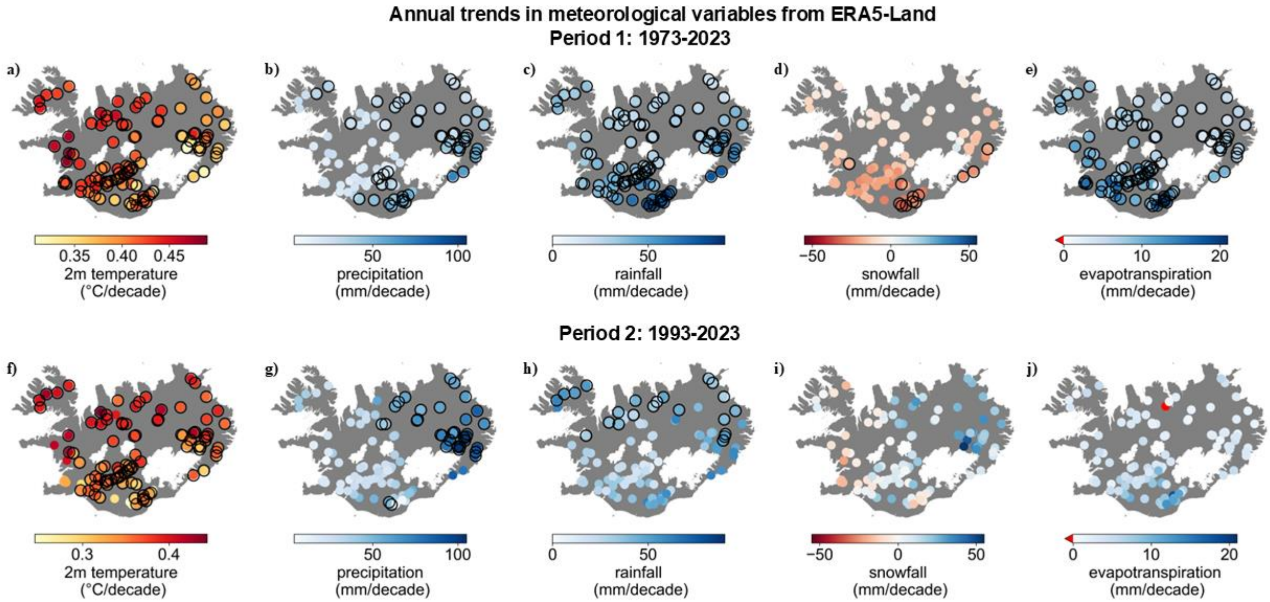

Figure S17: Trends in catchment-average temperature, precipitation, rainfall, snowfall and evapotranspiration from 1973-2023 and 1993-2023, with precipitation and evapotranspiration in the units of mm/decade. Panels a and f show temperature, b and g show precipitation, c and h show rainfall, d and i show snowfall, e and j show evapotranspiration, with each point marking the streamflow gauge location. Evapotranspiration trends are shown as percentage of annual precipitation per decade. Black circles around gauge markers indicate statistically significant trends ($p < 0.05$). The data is from the ERA5-Land reanalysis (Muñoz-Sabater et al., 2021)**.**

Figure S18 shows a comparison between trends in precipitation and ET in Iceland.

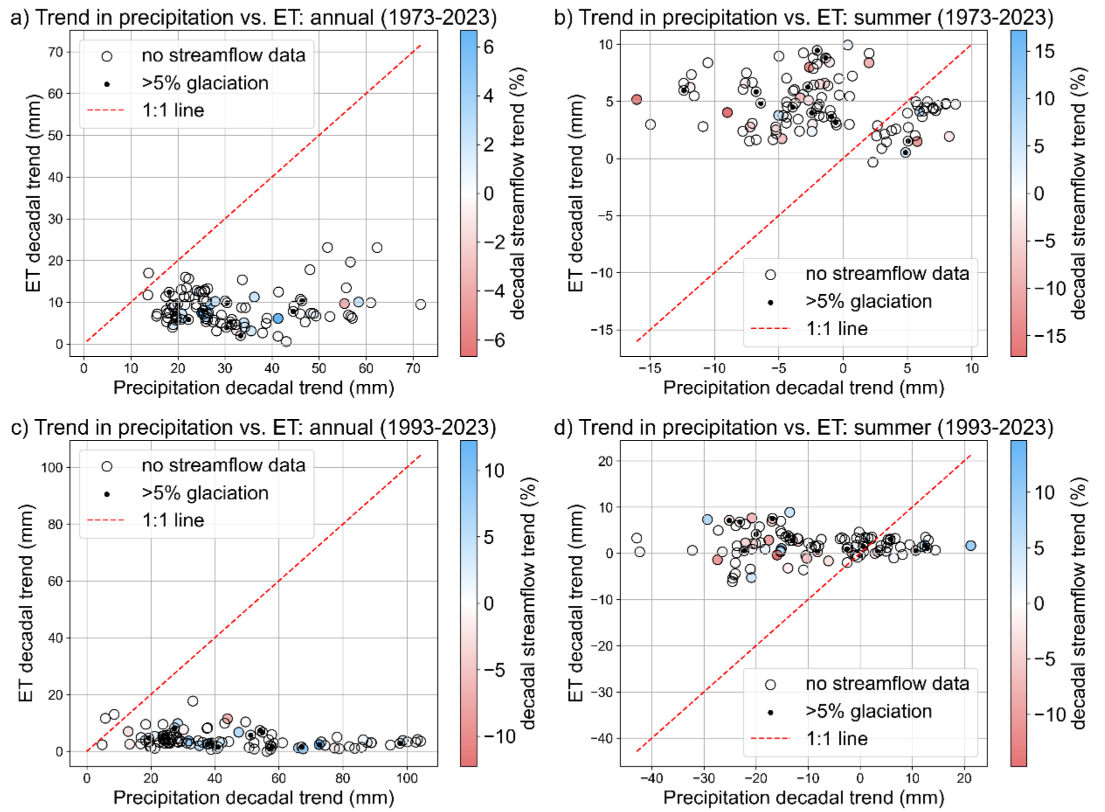

Figure S18: The trend in precipitation (x-axis) plotted against the trend for evapotranspiration (ET: y-axis) for period 1 (a and b) and period 2 (c and d). Annual trends are shown in panels a and c, summer trends (JJA) are shown in panels b and d. Colors indicate streamflow trends.

S3 Trends in streamflow

Figure S19 shows the streamflow, temperature and precipitation series for the 5 gauges in the northern part of Iceland showing a significant trend in annual average streamflow in period 1.

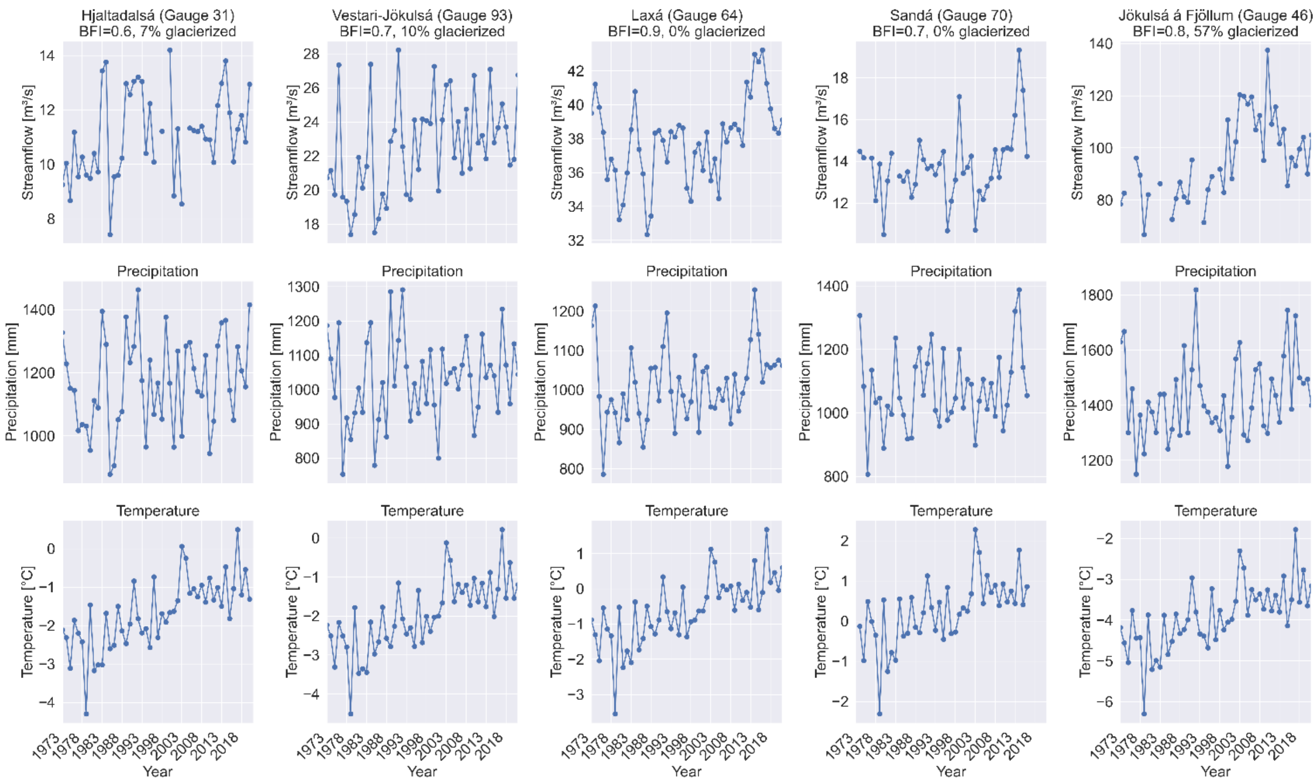

Figure S19: Annual average streamflow (top row), accumulated precipitation (middle row) and average temperature (bottom row) for the five gauges in northern Iceland showing statistically significant trends in streamflow during period 1. Each column corresponds to specific gauge, highlighting temporal changes in hydrological and meteorological variables over the analysis period. The name of the river, the gauge ID number, baseflow index (BFI) and percent glaciation of the catchment (Helgason and Nijssen, 2024) **is shown in the Figure Stitles in the top row. The gauges are arranged from left to right, progressing geographically from west to east.**

Figure S20 shows trends in annual and summer melt season streamflow in glacial rivers for periods 1 and 2.

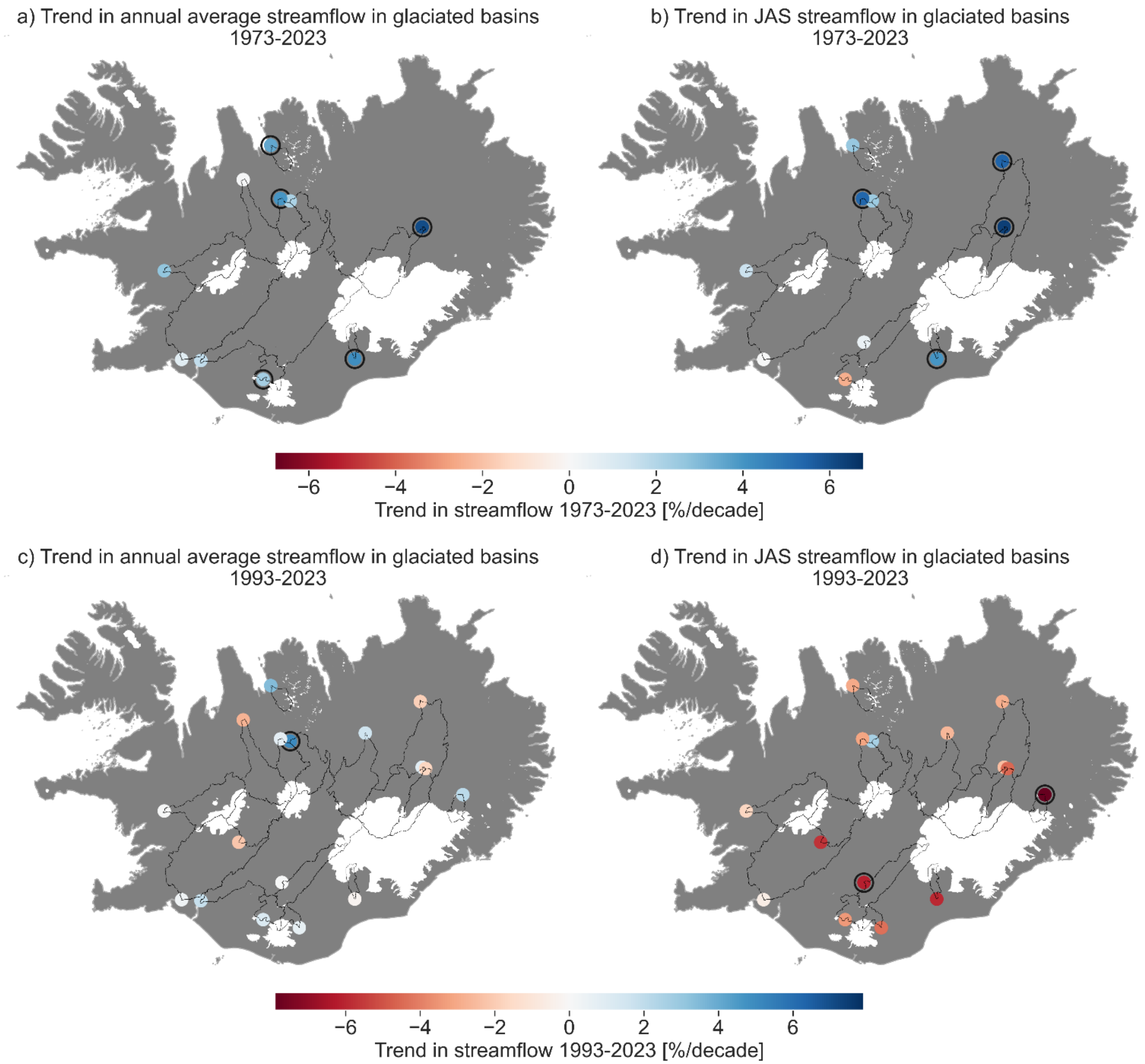

Figure S20: Trends in streamflow for gauges with more than 5% catchment glaciation. Annual trends (a, c) and summer melt season (July, August and September: b, d) in streamflow from 1973-2023 (a, b) and 1993-2023 (b, d). Black circles around gauge markers indicate statistically significant trends ($p < 0.05$). Watershed outlines are shown for each gauge.

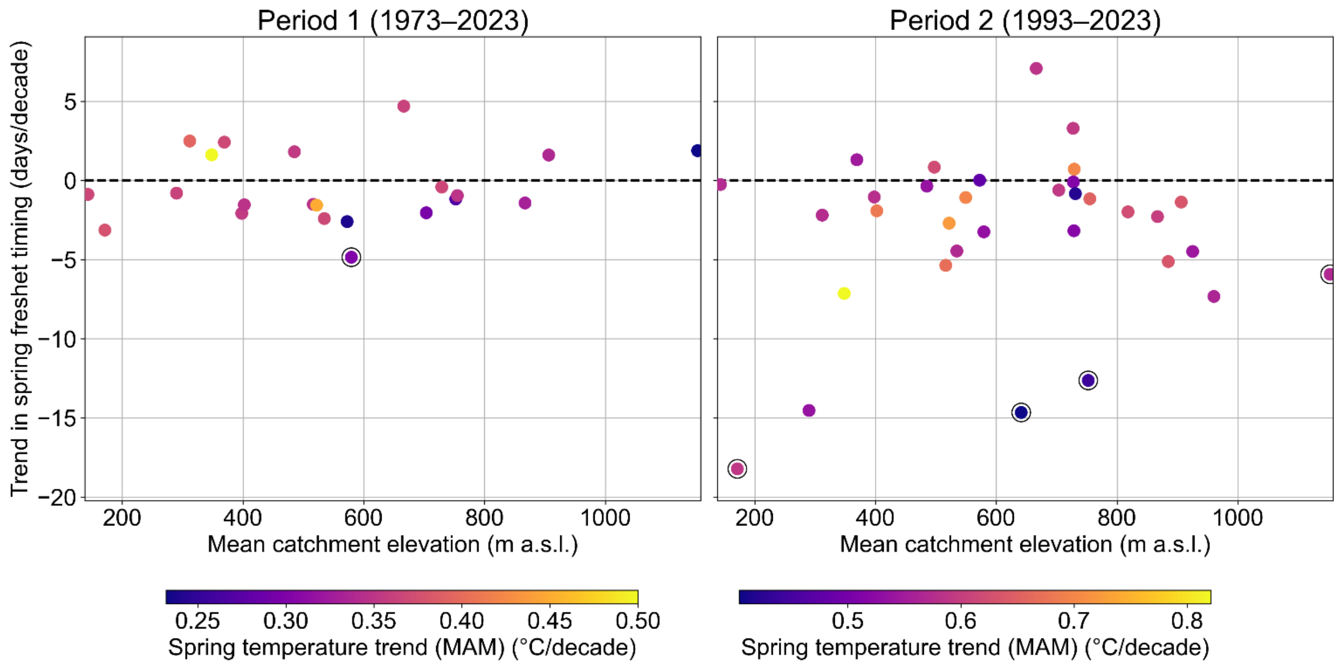

Figure S21: The trend in the timing of onset of spring freshet (y axis) vs. the mean catchment elevation for period 1 (a) and period 2 (b). Colors indicate the trend in spring temperature (MAM).

Tables S1 and S2 present streamflow trend results for periods 1 and 2.

Table S1: Streamflow trend results for period 1, 1973-2023. Unit of trends is %/decade.

id	Annual trend	annual_pval	trend_DJF	trend_MAM	trend_JJA	trend_SON
3	2.15	0.09	3.84	3.81	-1.83	7.16
7	0.09	0.95				
8	2.26	0.05	2.94	1.65	0.5	3.44
11	4.22	0.01	3.01	4.16	2.31	9.11
12	1.78	0.14	8.16	7.7	-4.23	5.17
14	1.25	0	0.14	2.78	0.57	2.42
18					-1.27	
21	3.34	0.09	9.95	5.48	-9	10.79
31	3.51	0	6.58	4.22	0.12	10.31

34	2.25	0.23	2.58	12.11	-2.44	8.25
37	2.65	0.16	4.37	2.16	-0.28	4.44
39	-3.98	0.11	-0.31	-2.83	-3.37	0
45					3.77	7.15
46	6.06	0.03	2.43	4.59	5.7	6.44
58	-0.28	0.95	1.85	0.52	-6.3	1.42
64	2.2	0.01	2.8	2.41	1.69	3.02
66	2.33	0.01	3.24	14.2	-4.3	7.47
67	-1.14	0.76	10.49	-1.99	-13.4	5.35
70	0.92	0.31	7.89	0.16	-2.42	3.91
79	0.55	0.52	0.7	1.01	0.28	2.72
82	1.81	0.25	3.01	2.97	-2.5	2.65
83	5.97	0	5.96	6.96	5.43	5.72
84	0.11	0.96	2.97	-1.31	-3.22	5.58
86					-1.53	6.4
91				-6.35	-4.77	
93	3.98	0.01	4.58	0.12	2.89	8.47
95	-0.29	0.94	0.59	1.07	-1.3	-0.61
98	0.78	0.41	2.06	0.95	-2.26	3.4
102	1.67	0.06				
105				-4.9	-8.83	-10.06

Table S2: Streamflow trend results for period 2, 1993-2023. Unit of trends is %/decade.

id	annual_trend	pval	trend_DJF	trend_MAM	trend_JJA	trend_SON
3	5.03	0.02	5.14	8.35	2.03	8.58
7	-2.77	0.3				
8	1.57	0.28	1.88	2.78	1.26	1.6

11	-0.23	1	-2.99	10.79	0.15	4.24
12	1.3	0.68	3.76	6.56	-2.87	4.68
14	2.61	0.12	0.15	5.17	6.18	3.15
15	6.76	0.12	14.47	26.48	-7.2	12.65
18	2.44	0.59	-6	-1.44	5.66	4.22
21	7.79	0.04	10.01	18.69	-5.89	13.29
26	-0.85	0.87	-13.37	-1.46	5.55	3.4
31	3.4	0.2	4.95	8.08	-0.28	6.88
34	0.03	1	-0.05	18.66	-3.15	3.97
36	-2.19	0.38	1.84	-2.8	-4.33	-0.94
37	0.03	1	1.28	0.34	-2.2	1.37
38	0.62	0.83	-4.24	6.32	-0.98	-1.62
39	1.39	0.8	0.46	3.91	-2.22	1.53
45	-1.9	0.48	-2.77	2.72	-1.24	2.75
46	0.94	0.83	4.39	4.43	-2.86	-1.51
48	2.15	0.54	5.39	6.74	-6.08	12.49
58	9.06	0.08	8.8	17.23	4.2	10.43
59	-1.69	0.57	-9.43	2.59	-2.88	7.24
64	4.55	0.01	4.01	3.44	5.02	6.26
66	1.14	0.56	-1.29	12.54	1.64	-0.1
67	-1.39	0.78	5.31	5.77	-11.05	0.86
70	3.52	0.18	7.4	1.59	-0.91	10.55
73					-5.54	
77	1.66	0.39	1.15	4.75	-1.4	1.73
79	2.21	0.47	1.77	2.9	1.82	3.82
82	9.94	0.02	5.6	13.17	8.99	10.55
83	7.88	0	7.98	9.55	7.45	7.96
84	-0.22	0.94	-0.88	-3.14	0.38	5.72

86	0.04	0.97	-3.9	8.06	-3.99	0.84
91	2.69	0.24	-5.72	-1.95	2.6	7
92	2.3	0.56	-7.18	7.38	1.89	-0.39
93	0.78	0.57	1.47	1.13	-0.6	1.83
98	0.31	0.75	1.3	2.16	-0.85	3.15
102	1.85	0.27				
105	-6.26	0.18	-18.12	4.91	-5.73	-4.03

S4 Overview of gauges used in the study

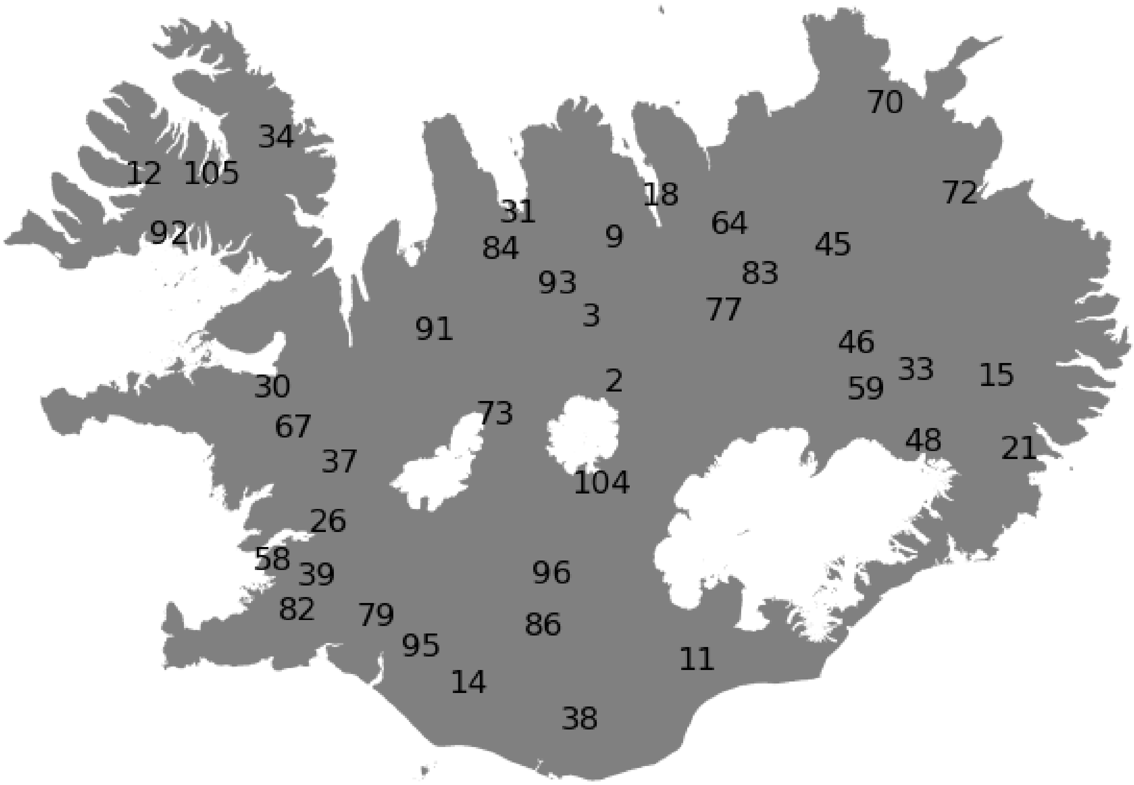

Figure S22: A map showing the location of streamflow gauges from the LamaH-Ice dataset used in the study. Gauges identified by their LamaH-Ice ID numbers.

Table S3: Overview of gauges used in this study, including river names, gauge locations, observation periods, and catchment attributes from the LamaH-Ice dataset: degree of anthropogenic impact (u: no influence, l: low influence, m: moderate influenc, s: strong influence), catchment glacier percentage, baseflow index (BFI – calculated with the method of Ladson et al. (2013)). These attributes are further explained in the paper describing the LamaH-Ice dataset (Helgason and Nijssen, 2024).

ID	River name	Station name	Degree of anthropogenic impact	Catchment glacier percentage	BFI	First year of observations	Last year of observatoins
3	Austari-Jökulsá	ofan Skatastaða	u	9	0.76	1971	2023

7	Blanda	Langamýri	s	10	0.79	1974	2023
8	Brúará	Dynjandi	l	0	0.88	1948	2023
11	Djúpá	neðan Djúpárdals	u	33	0.64	1968	2023
12	Dynjandisá	Sjóarfoss	l	0	0.63	1956	2023
14	Eystri-Rangá	Tungufoss	l	1	0.84	1962	2023
15	Fellsá	Sturluflöt II	u	0	0.44	1977	2023
18	Fnjóská	ofan Árbugsár	u	0	0.73	1976	2023
21	Fossá	Eyjólfsstaðir	u	0	0.38	1968	2023
26	Grímsá	Reyðarvatnsós	l	0	0.76	1964	2023
31	Hjaltadalsá	brú, Viðvíkursveit	u	7	0.59	1956	2023
34	Hvalá	Óp	u	0		1976	2023
36	Hvítá	Fremstaver	l	19	0.78	1985	2021
37	Hvítá	Kljáfoss	u	19	0.88	1951	2023
38	Hólmsá	Hólmsárfoss	u	21	0.79	1984	2023
39	Hólmsá	Gunnarshólmi	u	0	0.69	1972	2023
45	Jökulsá á Fjöllum	Grímsstaðir	u	29	0.74	1965	2023
46	Jökulsá á Fjöllum	Upptyppingar II	u	57	0.82	1972	2023
48	Jökulsá í Fljótsdal	Eyjabakkafoss	u	42	0.58	1985	2023
58	Korpa	Keldnaholt	l	0	0.62	1970	2023
59	Kreppa	Lónshnjúkur	u	36		1985	2023
64	Laxá	Helluvað	l	0	0.86	1961	2023
66	Markarfljót	Emstrur	u	10	0.66	1982	2023
67	Norðurá	Stekkur	u	0	0.45	1971	2023
70	Sandá	Flögubrú II	u	0	0.67	1965	2023
73	Seyðisá	Kjölur	u	2	0.63	1990	2023
77	Skjálfandafljót	Aldeyjarfoss	u	6	0.72	1987	2023
79	Sog	Ásgarður	m	1	0.9	1972	2023
82	Suðurá	Hófleðurshóll	u	0	0.82	1972	2023

83	Svartá	ofan Ullarfossbrúar	l	0	0.88	1965	2023
84	Svartá	Svartá	u	0	0.7	1932	2023
86	Tungnaá	Maríufoss	u	10	0.76	1959	2023
91	Vatnsdalsá	Forsæludalur	u	0	0.67	1948	2023
92	Vatnsdalsá	Eiði	l	0	0.55	1977	2023
93	Vestari-Jökulsá	Goðdalabrú	u	11	0.73	1971	2023
95	Ytri-Rangá	Árbæjarfoss	u	0	0.93	1961	2015
98	Ölfusá	Selfoss	l	11	0.82	1950	2023
102	Þjórsá	Þjórsártún	s	13	0.85	1947	2023
105	Þverá	Nauteyri	u	0	0.55	1967	2021

References

Fleig, A. K., Andreassen, L. M., Barfod, E., Haga, J., Haugen, L. E., Melvold, K., Hisdal, H., and Saloranta, T.: Norwegian Hydrological Reference Dataset for Climate Change Studies, Norwegian Water Resources and Energy Directorate, Oslo, Technical report, ISBN: 978-82-410-0869-6, 2013.

Helgason, H. B. and Nijssen, B.: LamaH-Ice: LArge-SaMple DAta for Hydrology and Environmental Sciences for Iceland, Earth Syst Sci Data, 16, 2741–2771, https://doi.org/10.5194/ESSD-16-2741-2024, 2024.

Hróðmarsson, H. B. and Þórarinsdóttir, T.: Flóð íslenskra vatnsfalla Flóðagreining rennslisraða, 2018.

Hussain, M. M., Mahmud, I., and Bari, S. H.: pyHomogeneity: A Python Package for Homogeneity Test of Time Series Data, J Open Res Softw, 11, https://doi.org/10.5334/JORS.427, 2023.

Ladson, A. R., Brown, R., Neal, B., and Nathan, R.: A standard approach to baseflow separation using the Lyne and Hollick filter, Australian Journal of Water Resources, 17, 25–34, https://doi.org/10.7158/W12-028.2013.17.1, 2013.

Muñoz-Sabater, J., Dutra, E., Agustí-Panareda, A., Albergel, C., Arduini, G., Balsamo, G., Boussetta, S., Choulga, M., Harrigan, S., Hersbach, H., Martens, B., Miralles, D. G., Piles, M., Rodríguez-Fernández, N. J., Zsoter, E., Buontempo, C., and Thépaut, J.-N.: ERA5-Land: a state-of-the-art global reanalysis dataset for land applications, Earth Syst. Sci. Data, 13, 4349–4383, https://doi.org/10.5194/essd-13-4349-2021, 2021.

Pettitt, A. N.: A Non-Parametric Approach to the Change-Point Problem, J R Stat Soc Ser C Appl Stat, 28, 126–135, https://doi.org/10.2307/2346729, 1979.